CrossMark

An improved three-dimensional multibody model of the human spine for vibrational investigations

Pier Paolo Valentini[1] · Ettore Pennestrì[1]

Abstract In this paper, a three dimensional numerical model of the human spine, specialized for vibrational investigations, is presented. The model has been built using multibody dynamics techniques and includes the entire set of vertebrae, considered as rigid bodies. The interaction between vertebrae has been simulated using six component bushings, without the need of any kinematic constraint. This methodology allows a very relevant flexibility, and the fully three-dimensional deformation modes of the spine may be studied. The investigation has been focused on the assessment of the vibration modes and the computation of the transmissibility functions buttocks-to-head for acceleration inputs along three main directions. It has been observed that the first torsional modes with a relevant mass participation factors are present at very low frequencies. Most of the relevant modes, which involve the deformation of the spine with relevant participation factor, are within the range 0÷5 Hz. These peaks are also visible in the transmissibility functions. Results have been also compared to those of other experimental and numerical studies.

Keywords Spine · Vibration · Multibody · Simulation · Human modelling

1 Introduction

The biofidelic numerical modelling of the human body is a very difficult task. On the one hand, there is the intrinsic complexity of the biomechanical behaviour of the anatomical structures; on the other hand, there is the high variability of the properties among the subjects. All these complications imply several simplifications and assumptions during the building of the numerical models. Moreover, especially in the biomechanical field, it is difficult to setup a model that can be suitable for different kinds of investigations since the building strategy has to be personalized for the actual purpose of the simulation.

✉ P.P. Valentini
valentini@ing.uniroma2.it

[1] Department of Enterprise Engineering, University of Rome "Tor Vergata", Via del Politecnico, 1, 00133, Rome, Italy

In the field of human vibrations and in particular for the evaluation of the risk of body exposure to vibration of machine interfaces, it is important to monitor three different factors: the duration, the amplitude and the frequency of the absorbed acceleration [1]. According to International standards such as ISO 2631 for the whole body vibration [2] and ISO 10819 for the hand–arm [3], the risk is assessed by the evaluation of acceleration signals at some important locations of the human body and the comparison to threshold values.

For these reasons, it is important that a biofidelic vibrational model of the human body provides an accurate simulation of the propagation of acceleration signals through the anatomical structures.

In the propagation of these vibration signals, the human spine plays a very interesting and crucial role. In both whole body vibration (seated, supine and stand up position) and hand–arm vibration, the spine represents the most important structural connection of the head to the rest of the body [4]. It is a specific path for delivering acceleration signal to the brain. This justifies the motivation for an accurate modelling of the spine complex suitable for different vibration studies.

Scientific literature reports many contributions on the building of such simulative tools using different approaches and levels of complexity. Besides the linear models [5], which are often used for preliminary assessment, the state-of-the-art in the development of these instruments is represented by finite element models and multibody dynamics models.

The most detailed and potentially accurate contributions are concerned with the development of finite element models. According to the scientific literature, they seem to be the preferred methodology for assessing static loading and stability [6]. They are also used in the vibration investigations, even if the modelling is often restricted to the two-dimensional behaviour in the sagittal plane or the modelling of the spine is often limited to the lumbar vertebrae. For example, Kitazaki and Griffin [7] proposed a two-dimensional finite element model of the whole spine based on beam elements and linear springs. Seidel et al. [8] proposed a plane symmetric finite element model of the lumbar spine. Another finite element model of the spine, limited to the lumbar segments, was proposed by Guo et al. [9]. Almost the same research group numerically evaluated the effect of an injured spine on the response to vertical vibration using a T12-pelvis finite element model [10] and the influence of anteroposterior shifting of trunk mass centroids [11]. Other authors implemented full body finite element models with more detailed substructuring of the spine [12, 13].

On the one hand, the finite element strategy allows a very accurate description of the biomechanical features, capable of assessing the mechanical stresses and deformation inside the structure, the local behaviour of the tissues. On the other hand, it is computationally demanding, and the identification of all the parameters in the model is a very hard task [14]. These features make this modelling strategy more suitable for a specific investigation rather than for developing a parametric model and for the inclusion in more complex simulative scenarios. Moreover, due to the necessity of the assessment of many local and specific parameters (both elastic and geometric), a robust identification and validation may be very complex [15, 16].

Other authors contributed to the development of multibody models. They allow for the definition of detailed mock-ups, including bony segments, compliant structures, three-dimensional nonlinear behaviour, but all the parameters are lumped and can be changed and optimized without the direct relationship to the geometry and morphology. Moreover, from a computational point of view, they are less onerous to be solved and can be easily integrated in a more complex simulative environment. As for the finite element approach, the vibrational models of the human spine are often limited to the simulation in the sagittal plane and with emphasis on the lumbar segments. As an example, Yoshimura et al. [17] presented a planar multibody model of the lumbar segment which has 10 degrees of freedom.

Another author worked on the definition of a full spine model including the contribution of all the vertebrae, but limited the vibrational motion in the sagittal plane [18]. Other authors also included the effect of muscles for the developing of generic numerical models suitable for different types of simulations [19]. A combination of the finite element and multibody approaches was studied by Verver at al. [20] by using the commercial MADYMO digital mannequin. More recently, Valentini [21] proposed a multibody condensed model of the human spine based on the development of a specific flexible element built using the dynamic spline theory [22].

Starting from this scientific background and contributions, the purpose of the paper is the development of a detailed multibody model of the human spine, suitable for vibrational investigation. The novelty of the model is that it includes the contribution of all the vertebrae, and it is able to mimic the three-dimensional motion of the spine. Moreover, due to the specific definition of the elastic compliance between bony segments, it does not possess any kinematic constraints which may limit the physiological degrees of freedom of the structure.

The paper is organized as follows. In the first part, the general idea behind the modelling strategy is presented. In the second part, the detailed model is introduced and discussed. In the third part, some interesting results are presented and compared with previous experimental and numerical contributions.

2 Modelling strategy of the interaction between vertebrae

The human spine consists of a set of discrete bony elements (vertebrae) connected by compliant structures such as ligaments, intervertebral disks and muscles. This combination of rigid and compliant bodies gives the spine great flexibility in the three-dimensional space, and the spine complex may accomplish different movements. The spine can be divided into four main regions. The cervical spine consists of seven vertebrae (C1, . . . , C7), and it supports the base of the skull. The thoracic spine consists of 12 vertebrae (T1, . . . , T12). The rib cage is connected to the thoracic vertebrae. The lumbar spine consists of five vertebrae (L1, . . . , L5). The sacrum and coccyx consist of five fused vertebrae each.

The mobility of the spine is due to the compliance between each functional spinal unit (FSU), comprising a superior vertebra, the intervertebral disc, the inferior vertebra, and the ligaments. The relative motion of two adjacent vertebrae has six degrees-of-freedom (axial, lateral and sagittal rotations and axial, lateral and antero–posterior translations).

The description of the flexibility between vertebrae plays a very important role in the accuracy and the capability of a simulative model. Some authors have proposed the use of a kinematic constraint (i.e. a revolute joint), located between spinous process, in order to limit the relative motion to a single degree of freedom (a rotation in the sagittal plane) [17, 22]. This simplification can be useful for including the most important field of motion in the whole-body vibration, but tends to neglect some other important degrees of freedom. Moreover, the actual relative axis of rotation between adjacent vertebrae depends on the applied loads, and imposing a revolute joint between them is equivalent to fixing its position in space. Especially in the small displacement region, such as required for studying the vibrations, it is important that the relative motion between two adjacent vertebrae possesses six degrees of freedom and an elasto-kinematic behaviour as most of the human joints [23].

Taking into account the elasticity and the mobility of all six degrees of freedom is quite complex. Experimental and numerical studies on a single FSU unveiled that the compliance and the mobility of an FSU can be efficiently simulated using a bushing element [24–26]. Following this approach, the interaction between two adjacent vertebrae i and $i-1$ (see

Fig. 1 Reference systems for the definition of the interaction between vertebrae
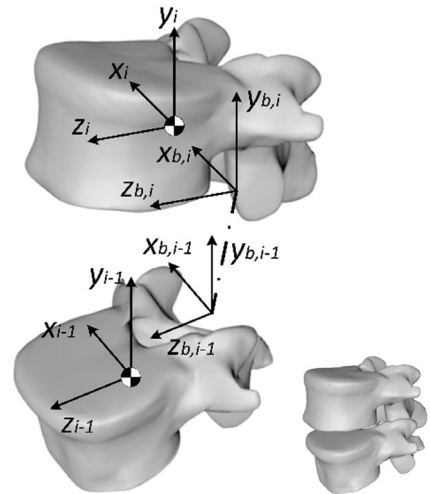

Fig. 1 for reference) can be simulated without kinematic constraints but using only a six-component force $F_{i,i-1}$, which can be evaluated using the formula

$$F_{i,i-1} = -[K]_{i,i-1}\{\delta\}_{i,i-1} - [C]_{i,i-1}\{\dot{\delta}\}_{i,i-1} \tag{1}$$

where

$[K]_{i,i-1}$ is the 6×6 stiffness matrix, with k_{ij} coefficients;
$[C]_{i,i-1}$ is the 6×6 damping matrix, with c_{ij} coefficients;
$\{\delta\}_{i,i-1}$ and $\{\dot{\delta}\}_{i,i-1}$ are the vectors of relative displacement and velocity, respectively, between the two bushing reference systems $\{O_{b,i} \ x_{b,i} \ y_{b,i} \ z_{b,i}\}^T$ and $\{O_{b,i-1} \ x_{b,i-1} \ y_{b,i-1} \ z_{b,i-1}\}^T$.

Actually, the choice of the location and the parameters of this bushing element may lead to diagonal or not diagonal stiffness matrices [25].

Each couple of adjacent vertebrae has its own bushing with the location of the reference systems and the corresponding stiffness and damping parameters. Since the complete spine has 24 vertebrae plus the head and the sacrum/coccyx complex, the whole model requires the definition of 26 bushing elements. A complete experimental evaluation of the entire set of parameters would require a very long measurement procedure, thus we decided to assign feasible values to each bushing, using the following strategies.

For the definition of the location and attitude of each bushing reference frame, we have:

1. The centre of each bushing (i.e. the origin of the $\{O_{b,i} \ x_{b,i} \ y_{b,i} \ z_{b,i}\}^T$ and $\{O_{b,i-1} \ x_{b,i-1} \ y_{b,i-1} \ z_{b,i-1}\}^T$ reference frames) is chosen according to [7] and [18]. Actually, the two papers deal with two-dimensional models, but due to the symmetry of a healthy spine, the origin can be located on the sagittal plane;
2. The $x_{b,i}$ and $x_{b,i-1}$ directions are set coincident to each other and normal to the sagittal plane;
3. The $y_{b,i}$ and $y_{b,i-1}$ directions are set coincident to each other and tangent to the curve that interpolates all the bushing centres, as determined in [21] pointing upward (from the sacrum to the head);
4. The $z_{b,i}$ and $z_{b,i-1}$ directions are set coincident to each other and perpendicular to the previous ones in order to form right-handed frames pointing forward.

For the definition of the stiffness parameters of each bushing reference frame, we have:

1. The k_{ij} ($i \neq j$) coefficients of the matrix are set to 0 since we adopt the diagonal bushing matrix as suggested in [25];
2. The k_{44} coefficients (i.e. the coefficients that describe the stiffness for the relative rotation about the $x_{b,i}$ or the $x_{b,i-1}$ axis) are set equal to the rotational springs of the model described in [18];
3. The other k_{ii} coefficients are set according to the ratio k_{ii}/k_{44} of the stiffness matrix in [27]. This choice is driven by the hypothesis that, due to the anatomical similitude of the compliant structures, the ratio between the stiffness coefficients of the matrix can be considered almost constant for all the vertebrae.

For the definition of damping coefficients, we have:

1. The c_{jk} ($j \neq k$) coefficients of the matrix are set to 0 since we adopt a diagonal matrix;
2. The c_{44} coefficients (i.e. the coefficients that describe the damping for the relative rotation about the $x_{b,i}$ or the $x_{b,i-1}$ axis) are set equal to the rotational damping elements of the model described in [18];
3. The other c_{jj} coefficients have been computed by imposing the same damping ratio in all the directions as

$$c_{jj} = c_{44} \frac{\sqrt{k_{jj} m_{jj}^{i,i-1}}}{\sqrt{k_{44} m_{44}^{i,i-1}}} \tag{2}$$

where $m_{jj}^{i,i-1}$ is the reduced mass element of the FSU of the vertebrae i and $i-1$, computed as

$$m_{jj}^{i,i-1} = \frac{m_{jj}^{i} \cdot m_{jj}^{i-1}}{m_{jj}^{i} + m_{jj}^{i-1}}. \tag{3}$$

The complete set of bushing parameters is reported in Table 1.

3 Multibody model of the spine

The complete multibody spine model is made of 33 rigid bodies: the head, 24 vertebrae, the sacrum/coccyx complex, and 7 visceral masses. The visceral masses are a discrete representation of the contribution of the viscera to the system. They are split from T11 to L5 in 7 contributions, as suggested by previous simulative approaches [7, 18]. All mass and inertial properties of the spine segments are taken from [28] for the lower vertebrae, and from [29] for the upper ones. All centre of mass locations of the spine segments, mass properties and location of visceral masses are taken from [18]. As suggested by other authors, the inertial properties and the location of the centre of mass of the thoracic vertebrae from T1 to T6 have been altered in order to take into account the contribution of the upper arms. In particular, the mass of the arms (0.755 kg each) has been equally subdivided from vertebra T1 to T6. Details of this alteration are the same reported in [7].

The model does not include any kinematic constraint. On the other hand, it includes 24 bushing elements between adjacent vertebrae, a bushing between the C1 and the head and a bushing between the sacrum/coccyx and the ground which are located and dimensioned according to the procedure explained in the previous section (see Table 1 for the details).

Table 1 Location, stiffness and damping parameters of the spine bushing included in the model

Bushing	Location of the centre			Stiffness coefficients						Damping coefficients					
	x mm	y mm	z mm	k_{11} N/mm	k_{22} N/mm	k_{33} N/mm	k_{44} Nm/rad	k_{55} Nm/rad	k_{66} Nm/rad	c_{11} Ns/m	c_{22} Ns/m	c_{33} Ns/m	c_{44} Nms/rad	c_{55} Nms/rad	c_{66} Nms/rad
Head–C1	0.0	802.5	25.7	275	550	275	400	568	268	2202	3114	2202	0.84	1.19	0.56
C1–C2	0.0	757.1	14.1	150	300	150	900	1278	603	697	1174	697	0.54	0.77	0.36
C2–C3	0.0	748.0	11.8	350	700	350	80	114	54	1058	1783	1058	0.16	0.23	0.11
C3–C4	0.0	732.9	7.9	380	760	380	100	142	67	1109	1869	1109	0.18	0.26	0.12
C4–C5	0.0	717.8	4.1	397	794	397	120	170	80	1092	1841	1092	0.19	0.27	0.13
C5–C6	0.0	702.5	0.2	483	967	483	160	227	107	1208	2038	1208	0.22	0.31	0.15
C6–C7	0.0	686.0	−4.0	507	1014	507	220	312	147	1248	2103	1248	0.26	0.37	0.17
C7–T1	0.0	670.4	−8.0	667	1334	667	370	525	248	1783	3005	1783	0.42	0.60	0.28
T1–T2	0.0	654.6	−12.0	350	700	350	140	199	94	1650	2780	1650	0.33	0.47	0.22
T2–T3	0.0	628.6	−21.8	600	1200	600	280	398	188	1990	3354	1990	0.43	0.61	0.29
T3–T4	0.0	603.0	−31.8	750	1500	750	420	596	281	2281	3845	2281	0.54	0.77	0.36
T4–T5	0.0	576.9	−41.8	1050	2100	1050	700	994	469	2633	4438	2633	0.68	0.97	0.46
T5–T6	0.0	550.7	−50.9	950	1900	950	700	994	469	2615	4407	2615	0.71	1.01	0.48
T6–T7	0.0	523.2	−58.6	900	1800	900	700	994	469	2545	4290	2545	0.71	1.01	0.48
T7–T8	0.0	498.0	−63.5	750	1500	750	700	994	469	1963	3309	1963	0.60	0.85	0.40
T8–T9	0.0	471.2	−66.5	750	1500	750	770	1093	516	1872	3155	1872	0.60	0.85	0.40
T9–T10	0.0	443.2	−67.6	750	1500	750	770	1093	516	1934	3260	1934	0.62	0.88	0.42
T10–T11	0.0	413.7	−60.7	750	1500	750	840	1193	563	2002	3373	2002	0.67	0.95	0.45
T11–T12	0.0	383.1	−64.9	750	1500	750	700	994	469	949	1599	949	0.29	0.41	0.19
T12–L1	0.0	353.1	−62.0	900	1800	900	630	895	422	1058	1783	1058	0.28	0.40	0.19
L1–L2	0.0	319.8	−59.1	1065	2130	1065	630	895	422	1069	1801	1069	0.26	0.37	0.17
L2–L3	0.0	283.6	−57.9	1000	2000	1000	630	895	422	1155	1947	1155	0.29	0.41	0.19
L3–L4	0.0	245.1	−61.2	1000	2000	1000	630	895	422	1314	2215	1314	0.33	0.47	0.22
L4–L5	0.0	204.6	−71.1	935	1870	935	570	795	375	1430	2410	1430	0.35	0.50	0.23
L5–sacrum	0.0	165.1	−84.2	735	1470	735	490	693	329	4201	7080	4201	0.41	0.58	0.27
Buttocks tissue	0	80.0	0.0	87	87	87	10	10	10	1.5	1.5	1.5	190	190	190

Fig. 2 The whole multibody model of the spine
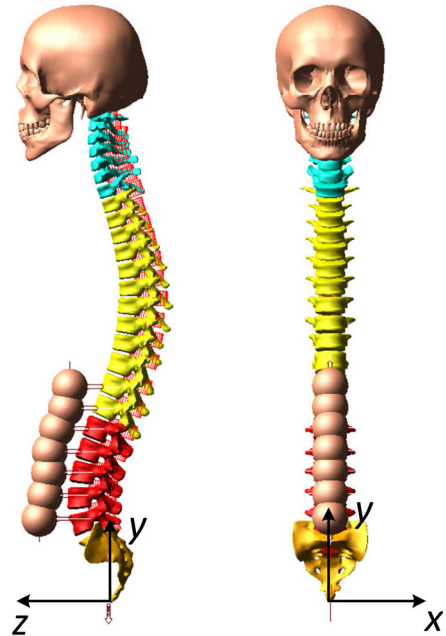
The model also includes other 7 bushing elements and 8 linear springs for describing the interaction between the vertebrae and the visceral masses. Each visceral mass is connected with a bushing element to the corresponding horizontal vertebra. The linear springs connect the centres of adjacent visceral masses (6 between visceral mass adjacent pair and two for between the upper and lower mass to the T10 and sacrum, respectively). The values of the horizontal (z, x) contributions to the stiffness and damping of the bushing elements are taken from [7]; no contribution to the rotational stiffness is considered. The vertical y compliance of the interaction between visceral masses has been symmetrically split between the vertical contribution of the bushing and the contribution of the linear springs. For this purpose, the vertical elastic compliance in [7] has been equally distributed between the bushing and the corresponding linear spring (as parallel spring contribution).

Another bushing element is included to simulate the elastic compliance of the buttocks tissue. The stiffness values are chosen according to those proposed in [7].

The whole model is depicted in Fig. 2, in both lateral and frontal view; the main reference frame is also indicated.

In order to assess the vibrational behaviour, two types of investigations have been carried out. The first one is the computation of the vibrational modes, obtained through the linearization of the equations of motion. The second investigation is about the computation of the acceleration transmissibilities from the buttocks to the head. In order to take into account the nonlinearities of the model, the transmissibility functions have been computed by imposing a series of sinusoidal inputs of acceleration at the buttocks, with variable frequency but same amplitude.

4 Vibration modes

The linearization of the equations of motion allows for the assessment of the natural frequencies of the spine system and the corresponding three dimensional modes. All the modes have

Fig. 3 Lower frequency modes due to buttocks compliance: first torsional mode at 0.27 Hz, *on the left*, first bending mode in the sagittal plane at 0.34 Hz, *in the middle* and first bending mode out of the sagittal plane at 0.39 Hz, *on the right*. Deformed shapes have been depicted in *red*, superimposed to the undeformed ones (Color figure online)
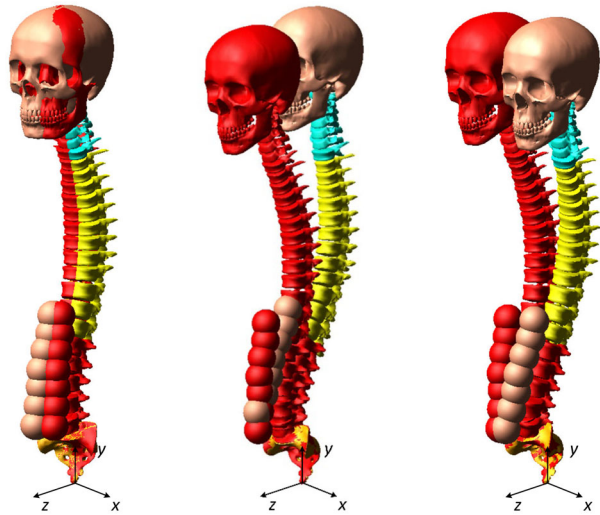
been computed neglecting the contribution of the damping coefficients in order to simplify the computation and avoid the presence of imaginary eigenvalues.

It has been observed that the first torsional modes with a relevant mass participation factors are present at very low frequencies. A mode has been considered relevant if the associated mass participation factor is at least 20 % higher than the mean between all the participation factors. The first torsional mode about the y axis appears at 0.27 Hz, the first bending mode about the z axis appears at 0.34 Hz and the first bending mode about the x axis appears at 0.39 Hz (see Fig. 3). All these modes are related to a displacement of the entire spinal complex with respect to buttocks, due to the lower stiffness of the corresponding elastic bushing.

Most of the relevant modes, which involve the deformation of the spine with relevant participation factor, are within the range 0÷5 Hz (see Fig. 4). The most relevant vertical mode is at 4.7 Hz, and it is characterized by bending deflection of the vertebrae. Another relevant vertical mode is found at 6.8 Hz, and it is also characterized by bending deflection. At about 15.7 Hz, another relevant vertical mode is computed, and it involves the axial translation.

Within the range of 0÷5 Hz, vertical secondary modes are often coupled with torsion and bending, especially of the cervical portion, due to the lower stiffness with respect to the thoracic one.

5 Acceleration transmissibilities

Three acceleration transmissibility curves of the buttocks–head channel have been evaluated. All of them have been computed by imposing a periodic acceleration with variable frequency v at the buttocks interface and measuring the corresponding acceleration at the head centre of mass. By this way, the transmissibility functions have been evaluated by points. Each point on the transmissibility function ($TR_{i-j}(v)$) has been computed as the ratio between the maximum amplitude of the acceleration at the head and that of the excitation:

$$TR_{i-j}(v) = \frac{|a(v)_{i,\text{head}}|}{|a(v)_{j,\text{excitation}}|} \tag{4}$$

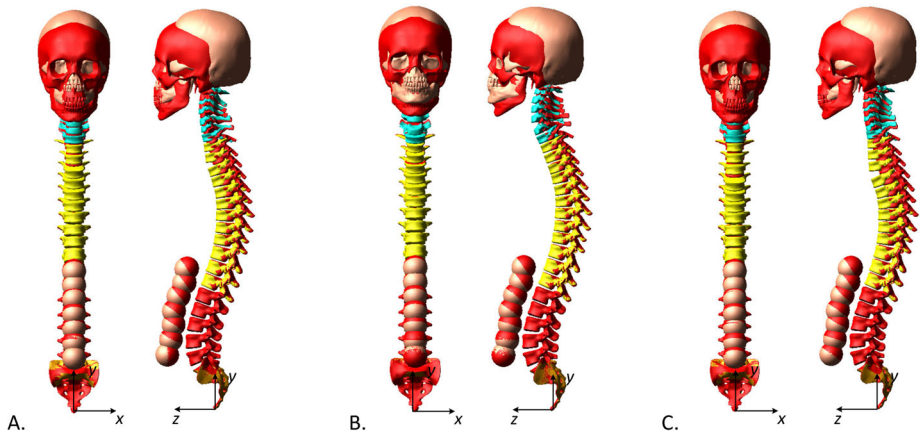where i and j are the measurement channels, i.e. (x y z Rx Ry Rz).

Fig. 4 Relevant vibrational modes in the sagittal plane: main bending mode at 4.7 Hz (A, *on the left*), secondary bending mode at 6.8 Hz (B, *in the middle*), translational mode at 15.7 (C, *on the right*). Deformed shapes have been depicted in *red*, superimposed to the undeformed ones (Color figure online)

Fig. 5 Vertical transmissibility $TR_{y-y}(\nu)$ from buttocks to head, built with 40 different simulation runs with different acceleration frequency (0.5 Hz spacing)
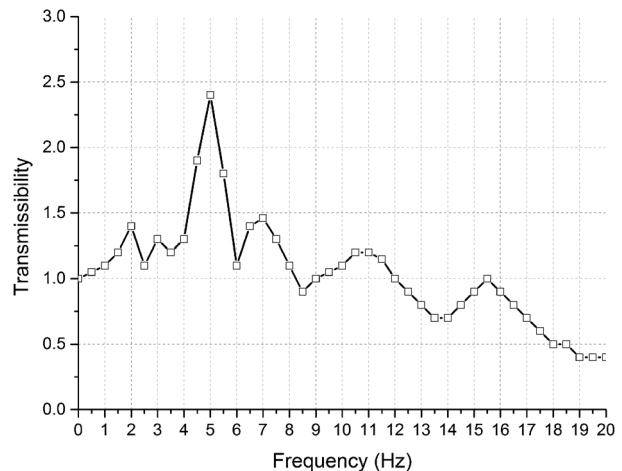
This method allows for taking into account the nonlinearities effects since each point is obtained imposing a specific amplitude [18] without the linearization of the mass and stiffness matrices.

The amplitude of the excitation has been chosen according to the equivalent acceleration $A(8)$ stated in the European Directive 2002/44/CE and equal to 1.15 m/s². The $A(8)$ acceleration is the limit for the absorbed vibration during an exposure of eight hours.

Forty equally-spaced transmissibility points in the range 0÷20 Hz have been computed for each curve.

Figure 5 shows the transmissibility of the vertical channel y, $TR_{y-y}(\nu)$. It is clear to observe that the curve presents two small peaks at 2.0 Hz and 3.0 Hz in which a limited amplification of the acceleration signal is reported. A higher peak appears around 5.0 Hz, in correspondence of the most relevant bending mode about the x axis. Another lower peak

Fig. 6 Fore-and-aft transmissibility $TR_{z-z}(\nu)$ from buttocks to head, built with 40 different simulation runs with different acceleration frequency (0.5 Hz spacing)
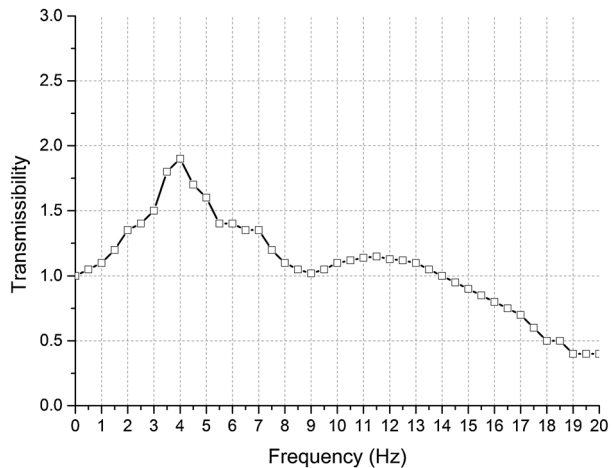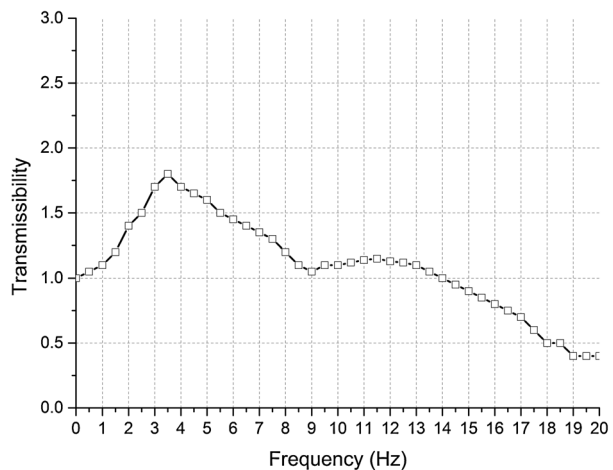

Fig. 7 Lateral transmissibility $TR_{z-z}(\nu)$ from buttocks to head, built with 40 different simulation runs with different acceleration frequency (0.5 Hz spacing)

appears near 7.0 Hz and a smaller one at 10.5 Hz. Another smaller peak occurs at 15.5 Hz. This last one is mainly due to the first vertical translational resonance frequency.

Figure 6 shows the transmissibility curve of the fore-and-aft (horizontal) channel z, $TR_{z-z}(\nu)$. In this case the main amplification is restricted in the range 0÷5 Hz and the amplitude is lower than that of the vertical channel. It is noticed a slightly shift towards lower frequencies (about 1.0 Hz) of the main peaks. The transmissibility levels are, for the entire region under investigation, lower than that for the vertical channel.

Figure 7 shows the transmissibility curve of the lateral channel x, $TR_{x-x}(\nu)$. It shows a similar trend with respect to that of the fore-and-aft channel. The peak is shifted of about 0.5 Hz towards the lower frequencies and the maximum amplification is a little bit lower than that for the horizontal channel.

6 Discussion

Concerning the natural frequencies, the relevant modes in the sagittal plane have been compared to those of other numerical contributions [7, 18], and the results are very close among

all the different considered models. In particular, Kitazaki and Griffin [7] reported a first mode at 0.28 Hz, and that computed with the proposed model is 0.27 Hz. The main bending mode of Kitazaki and Griffin is 5.06 Hz, and that of the proposed model 4.7 Hz. The value of 4.7 Hz is also confirmed by the multibody 2D model of Valentini [18]. Concerning the vibration modes out of the sagittal plane, no detailed comparisons are available, to the authors' best knowledge.

Concerning the transmissibilities, the vertical transmissibility curve has been compared to those of other contributions, both experimental [1] and numerical [7, 18]. The results, even in this case, are very close both in terms of frequency peak and corresponding amplification. In particular, Kitazaki and Griffin [7] reported the first peaks at 1.5 Hz, 2.8 Hz and 5.0 Hz that are in line with the peaks at about 1.8, 3.0 and 5.0 Hz computed by the proposed model. Valentini [18] also reported a peak at about 2.0 Hz and another at 4.4 Hz. Experimental investigations such as those collected in [1] also confirm a higher peak at about 4÷5 Hz (values are spread trough subjects).

Both horizontal and fore-and-aft transmissibility curves are consistent with the experimental observations in [30] and on the vibrational comfort assessment of different authors discussed and reviewed in [1] which shows main peaks in the range 3÷4 Hz with a lower amplitude with respect to the vertical one. To the authors' best knowledge, no direct numerical studies exist for direct comparison among simulative models in the horizontal and fore-and-aft directions.

According to the comparison to both experimental and other numerical models, the behaviour of the proposed model seems congruent. Due to the specific modelling strategy which involves all the discussed simplifications and assumptions, the model has also some limitations. The first is that it can reproduce the vibrational dynamics of the spine complex but it is not suitable for a direct assessment of internal loads. The description using force field elements such as bushings does not allow for the separation of intervertebral disk loads, joint loads and soft tissue loads. The second limitation is that the model is focused on low amplitude vibration, and it is not suitable for crash tests or impact dynamics due to the simplification in spine kinematics and properties of elastic elements.

7 Conclusion

A three-dimensional multibody model simulating the human spine and suitable for vibrational investigation has been presented. The model comprises all the 24 vertebrae, the head, the sacrum/coccyx, and the contribution of visceral masses. The model does not include any kinematic constraint but, in order to preserve the physiological compliance between the bony structures, the interaction between adjacent bodies has been simulated using six-component bushing elements. These elements are able to describe the stiffness along three directions and about three rotation axes between connected parts using six independent parameters. This modelling strategy is closer to the actual elasto-kinematic behaviour of the human tissue compared to the use of a kinematic constraint and a single-component spring.

The model predicts the main vibrational modes, and most of the results have been compared and are in good agreement with those coming from experiments and other numerical models. Moreover, the three dimensionality of the movement showed that, in the relevant range of the frequency for vibrational comfort, the bending and axial modes are often coupled with torsional modes especially of the cervical portion.

The computation of the transmissibility functions confirms that the vertical vibrations are more amplified than those along lateral and fore-and-aft directions. Moreover, the peaks of

the acceleration transmissibility of the vertical channel appear at frequencies slightly higher than those along the other two directions.

The proposed model can be considered as a detailed tool for performing numerical simulations and assessment of human vibration and for the computation of vibrational comfort of both seated and standing humans. Due to the limited number of degrees of freedom with respect to finite element models and due to the lumped parameters, it can be also embodied in other more complex scenarios, including full vehicle interiors/exteriors and interface environments (seat, backrest).

References

1. Griffin, M.J.: Handbook of Human Vibration. Academic Press, San Diego (1990)
2. International Organization for Standardization: ISO 2631-1 Mechanical Vibration and Shock-Evaluation of Human Exposure to Whole-body Vibration—Part 5: Method for Evaluation of Vibration Containing Multiple Shocks (2004)
3. International Organization for Standardization: ISO 10819 Mechanical vibration and shock—Hand-arm vibration—Measurement and evaluation of the vibration transmissibility of gloves at the palm of the hand (2013)
4. Seidel, H.: On the relationship between whole-body vibration exposure and spinal health risk. Ind. Health **43**, 361–377 (2005)
5. Liang, C.-C., Chiang, C.F.: A study on biodynamic models of seated human subjects exposed to vertical vibration. Int. J. Ind. Ergon. **36**, 869–890 (2006)
6. Schmidt, H., Galbusera, F., Rohlmann, A., Shirazi-Adl, A.: What have we learned from finite element model studies of lumbar intervertebral discs in the past four decades? J. Biomech. **46**, 2342–2355 (2013)
7. Kitazaki, S., Griffin, M.J.: A modal analysis of the whole-body vertical vibration using a finite element model of the human body. J. Sound Vib. **200**(1), 83–103 (1997)
8. Seidel, H., Blüthner, R., Hinz, B.: Application of finite-element models to predict forces acting on the lumbar spine during whole-body vibration. Clin. Biomech. **16**(1), s57–s63 (2001)
9. Guo, L.-X., Zhang, Y.-M., Zhang, M.: Finite element modeling and modal analysis of the human spine vibration configuration. IEEE Trans. Biomed. Eng. **58**(10), 2987–2990 (2011)
10. Guo, L.-X., Zhang, M., Zhang, Y.-M., Teo, E.-C.: Vibration modes of injured spine at resonant frequencies under vertical vibration. Spine **34**(19), E682–E688 (2009)
11. Guo, L.-X., Zhang, M., Wang Zhang, Y.-M., Wen, B.-C., Lid, J.-L.: Influence of anteroposterior shifting of trunk mass centroid on vibrational configuration of human spine. Comput. Biol. Med. **38**, 146–151 (2008)
12. Pankoke, S., Hofmann, J., Wölfel, H.P.: Determination of vibration related spinal loads by numerical simulation. Clin. Biomech. **1**, S46–S46 (2001)
13. Seidel, H., Hinz, B., Hofmann, J., Menzel, G.: Intraspinal forces and health risk caused by whole-body vibration—Predictions for European drivers and different field conditions. Int. J. Ind. Ergon. **38**, 856–867 (2008)
14. Pennestrì, E., Valentini, P.P., Vita, L.: Comfort analysis of car occupant: comparison between multibody and finite element models. Int. J. Veh. Syst. Model. Test. **1**(1/2/3), 68–78 (2005)
15. Noaillya, J., Wilke, H.-J., Josep Planella, A., Lacroixa, D.: How does the geometry affect the internal biomechanics of a lumbar spine bi-segment finite element model? Consequences on the validation process. J. Biomech. **40**, 2414–2425 (2007)
16. Niemeyer, F., Wilke, H.-J., Schmidt, H.: Geometry strongly influences the response of numerical models of the lumbar spine—A probabilistic finite element analysis. J. Biomech. **45**, 1414–1423 (2012)
17. Yoshimura, T., Nakai, K., Tamaoki, G.: Multi-body dynamics modelling of seated human body under exposure to whole-body vibration. Ind. Health **43**, 441–447 (2005)
18. Valentini, P.P.: Virtual dummy with spine model for automotive vibrational comfort analysis. Int. J. Veh. Des. **51**(3/4), 261–277 (2009)
19. de Zee, M., Hansen, L., Wong, C., Rasmussen, J., Simonsen, E.B.: A generic detailed rigid-body lumbar spine model. J. Biomech. **40**, 1219–1227 (2007)
20. Verver, M.M., van Hoof, J., Oomens, C.W.J., van de Wouw, N., Wismans, J.S.H.M.: Estimation of spinal loading in vertical vibrations by numerical simulation. Clin. Biomech. **18**, 800–811 (2003)
21. Valentini, P.P.: Modelling human spine using dynamic spline approach for vibrational simulation. J. Sound Vib. **331**, 5895–5909 (2012)

22. Valentini, P.P., Pennestrì, E.: Modelling elastic beams using dynamic splines. Multibody Syst. Dyn. **25**(3), 271–284 (2011)
23. Kecskeméthy, A., Weinberg, A.: An improved elasto-kinematic model of the human forearm for biofidelic medical diagnosis. Multibody Syst. Dyn. **14**(1), 1–21 (2005)
24. Gardner-Morse, M.G., Stokes, I.A.F.: Structural behavior of human lumbar spinal motion segments. J. Biomech. **37**, 205–212 (2004)
25. Christophy, M., Curtin, M., Senan, N.A.F., Lotz, J.C., O'Reilly, O.M.: On the modelling of the intervertebral joint in multibody models for the spine. Multibody Syst. Dyn. **30**, 413–432 (2013)
26. Abouhossein, A., Weisse, B., Ferguson, S.J.: A multibody modelling approach to determine load sharing between passive elements of the lumbar spine. Comput. Methods Biomech. Biomed. Eng. **14**(6), 527–537 (2011)
27. O'Reilly, O.M., Metzger, M.F., Buckley, J.M., Moody, D.A., Lotz, J.C.: On the stiffness matrix of the intervertebral joint: application to disk replacement. J. Biomech. Eng. **131**(8), 081007 (2009)
28. Christophy, M., Senan, N.A.F., Lotz, J.C., O'Reilly, O.M.: A Musculoskeletal model for the lumbar spine. Biomech. Model. Mechanobiol. **11**, 19–34 (2012)
29. Walker, L.B., Harris, E.H., Pontius, U.R.: Mass, volume, center of mass, and mass moment of inertia of head and head and neck of human body. Stapp Car Crash J. **17**, 535–537 (1973). SAE 730985
30. Mandapurama, S., Rakhejaa, S., Boileaub, P.-E., Maedac, S.: Apparent mass and head vibration transmission responses of seated body to three translational axis vibration. Int. J. Ind. Ergon. **42**(3), 268–277 (2012)